



Synergistic effects of iron oxide nanoparticles and indole-3-acetic acid on the germination and development of cold-stored chrysanthemum synthetic seeds

Dariusz Kulus¹ · Alicja Tymoszek¹ · Alicja Kulpińska¹ · Magdalena Osial²

Received: 26 September 2024 / Accepted: 20 December 2024
© The Author(s), under exclusive licence to Springer Nature B.V. 2025

Abstract

Iron oxide nanoparticles and indole-3-acetic acid are finding increasingly widespread applications in horticulture and plant biotechnology. They may be particularly useful in producing synthetic seeds, especially for species with high levels of self-incompatibility and heterozygosity, such as chrysanthemum - one of the most popular ornamental species on the floricultural market. The aim of this study was to verify the effects of iron oxide nanoparticles and indole-3-acetic acid on the germination of synthetic seeds and growth of chrysanthemum plants. Axillary buds of chrysanthemum (*Chrysanthemum × morifolium* / Ramat./ Hemsli.) 'Richmond' were embedded in a 3% calcium alginate solution prepared with Murashige and Skoog medium supplemented with indole-3-acetic acid (IAA) and/or iron oxide nanoparticles in pure form (Fe₃O₄ NPs) or stabilized/coated with citrate (Fe₃O₄CA NPs). NPs were synthesized using the modified wet co-precipitation method. The prepared synthetic seeds were stored for two months in darkness at 4 °C on Petri dishes filled with sterile agar-solidified water. For the next 30 days, the seeds germinated in a growth room under a 16-hour photoperiod (22 °C), and were then planted in a greenhouse in multi-pots filled with a peat and perlite mixture (2:1). The highest germination efficiency (86%) was achieved with the simultaneous addition of IAA and Fe₃O₄CA NPs to the alginate coating, while the lowest was observed in the control without IAA or NPs (47%). Fe₃O₄CA NPs (with or without IAA) stimulated the development of the longest shoots. No effect of iron oxide nanoparticles on rooting efficiency was observed, but IAA stimulated root elongation. The highest acclimatization efficiency (63%) was achieved by simultaneously adding IAA and Fe₃O₄CA NPs to the alginate coating (control survival rate was 19%). The presence of nanoparticles alone affected the content of flavonoids (increase) and anthocyanins (decrease) in plants, although not of chlorophyll. Measurements of fluorescence parameters confirmed the good health status of the plants and their photosynthetic efficiency, despite some stress caused by nanoparticles. No phenotypic variation during flowering was detected. This study confirms the usefulness of iron oxide nanoparticles and indole-3-acetic acid in the production and storage of synthetic seeds of chrysanthemum.

Key message

Iron oxide nanoparticles and indole-3-acetic acid enhance germination and growth of cold-stored synthetic seeds in chrysanthemum, improving acclimatization and metabolic profiles, while ensuring phenotype uniformity and plant health.

Keywords Alginate encapsulation · Chlorophyll fluorescence · Floriculture · Horticulture · Metabolites · Stress

Introduction

Nanotechnology is a promising field in horticulture and plant biotechnology, offering innovative solutions to enhance plant growth, development, and stress tolerance (Fraceto et al. 2016). Among numerous nanomaterials being explored, iron nanoparticles (NPs) in various forms (Fe NPs, Fe₂O₃ NPs, Fe₃O₄ NPs) have drawn significant attention due to their

Communicated by Nhut Tan Duong.

Extended author information available on the last page of the article

unique properties and potential applications in agriculture (Tawfik et al. 2021; Sun et al. 2022). These nanoparticles can serve as efficient sources of iron for plants, releasing the micronutrient under various pH conditions. Iron is an essential mineral for all living organisms. In plants, it is involved in numerous growth and biological processes, such as DNA synthesis, respiration, and photosynthesis (Zaid et al. 2020).

Recent studies have demonstrated the beneficial effects of iron oxide nanoparticles on various plant species, including improved growth parameters, enhanced photosynthetic pigment content, and increased antioxidant enzyme activities (Ahmed et al. 2023; Feng et al. 2022; Tawfik et al. 2021). Priming with Fe₂O₃ NPs enhanced germination of seeds and seedling growth in sorghum (*Sorghum bicolor* (L.) Moench) (Maswada et al. 2018) and wheat (*Triticum aestivum* L.) (Sundaria et al. 2019). El-Desouky et al. (2021) found that Fe₂O₃ NPs stimulated more efficient yield production in tomato (*Solanum lycopersicum* L.) compared to ferric chloride (FeCl₃) and EDTA-Fe by increasing photosynthate accumulation and translocation. Li et al. (2020) reported that Fe₂O₃ NPs increased the net photosynthesis rate, chlorophyll content, and biomass by 27.5%, 26.1%, and 34.6% in maize (*Zea mays* L.), respectively. However, the beneficial effect of iron NPs on plants is not always observed. According to Kasote et al. (2019), Fe NPs priming did not affect seed germination, seedling growth, and biosynthesis of chlorophyll in watermelon (*Citrullus lanatus* (Thunb.) Mansf.).

On the other hand, plant growth regulators, such as indole-3-acetic acid (IAA), continue to play a crucial role in plant biotechnology. IAA, a naturally occurring auxin, is predominantly produced in cells of the apical bud and very young leaves. This tryptophan derivative is known to promote plant growth and development, including cell elongation, proliferation, and differentiation (Zhao et al., 2010). The application of IAA has been shown to stimulate root development and overall plant growth in numerous ornamental species, both in vitro and in vivo (Abu-Zahra et al. 2013). For example, exogenous IAA application improved various growth parameters; i.e. stem diameter, plant height, leaf number, and leaf area; in *Syringa villosa* Vahl. (Jin et al. 2023). This treatment also enhanced the overall plant quality by increasing the contents of endogenous gibberellic acid (GA₃) and IAA, while reducing abscisic acid (ABA) levels. Additionally, IAA promoted photosynthetic capacity, evidenced by increased net photosynthetic rate, stomatal conductance, and transpiration rate (Jin et al. 2023). The combination of nanoparticles and plant growth regulators could be a good method for enhancing plant propagation techniques (Karakecili et al., 2019), particularly in the production of synthetic seeds.

Synthetic seed technology, which involves encapsulating explants in a protective coating, offers numerous advantages in plant propagation and conservation. It allows for

the storage and transport of plant material while maintaining viability and genetic integrity (Gentait et al., 2015). This approach is particularly valuable for species that exhibit high levels of self-incompatibility and heterozygosity, such as chrysanthemum (*Chrysanthemum × morifolium* Ramat./Hemsl.), one of the most economically valuable ornamental plants in the global floriculture market (Miler and Woźny, 2021). The incorporation of nanoparticles and growth regulators into the encapsulation matrix could potentially enhance the performance of synthetic seeds, improving germination rates, plant growth, and overall survival. To date, however, no studies on the application of nanoparticles in synthetic seed storage exist.

In previous studies with chrysanthemum micropropagation, we have used an increased by half content of iron by adding 13.9 mg·L⁻¹ FeSO₄·7H₂O and 20.6 mg·L⁻¹ Na₂EDTA·2H₂O into the standard MS medium or alginate coating (Jerzy et al. 2015; Kulus and Zalewska 2014). Here, instead of using additional iron in the bulk form, we added an equivalent concentration of this microelement in the form of Fe₃O₄ nanoparticles, assuming that micronutrients in nanoscale size are more accessible to plants than their larger counterparts, due to unique physicochemical properties, better penetration and easier transport within the plant (Wang et al. 2023).

This study aims to evaluate the impact of IAA and Fe₃O₄ NPs (both in pure form and stabilized with citrate) on the germination, growth, and acclimatization of chrysanthemum plants derived from cold-stored synthetic seeds, with the ultimate goal of enhancing propagation efficiency in this horticulturally significant crop. Given the potential benefits of both IAA and iron oxide nanoparticles in plant growth and development, the scientific hypothesis assumed a positive impact of the studied compounds on the overall performance of synthetic seeds.

Materials and methods

Nanoparticles were synthesized and characterized at the Institute of Fundamental Technological Research, Polish Academy of Sciences. The experiment on plants was performed in the Laboratory of Horticulture and Greenhouse of the Faculty of Agriculture and Biotechnology, Bydgoszcz University of Science and Technology (42°9'6.768" N, 18°0'29.27195" E), July 2023 – August 2024.

Synthesis of iron oxide nanoparticles

Iron oxide nanoparticles were synthesized using the wet co-precipitation method from the solution containing the source of Fe³⁺ and Fe²⁺ ions adapting the procedure presented in (Thanh et al. 2022). The synthesis was performed as follows:

1080 mg of iron chloride (III) hexahydrate $\text{FeCl}_3 \cdot 6\text{H}_2\text{O}$ (analytical grade, Warchem, Warsaw, Poland) was dissolved in 50 mL of distilled water (HYDROLAB water filtering system, Gliwice, Poland) and the solution was stirred magnetically with a magnetic bar at 600 rpm at room temperature. Next, 1 mL of 0.1 M HCl and 400 mg of iron chloride (II) tetrahydrate $\text{FeCl}_2 \cdot 4\text{H}_2\text{O}$ (analytical grade, Warchem) were added and dissolved with continuous stirring. When the salts were fully dissolved, the temperature of the solution was increased to 60 °C and 25% aqueous ammonia solution (Warchem) as the precipitating agent was added dropwise to adjust pH 11. The suspension was stirred continuously with heating on the hot plate for 30 min. After the synthesis, the beaker was placed onto the magnet to collect NPs onto the bottom of the beaker, remove the supernatant, and replace it with distilled water. Washing was repeated several times with vortex mixing to neutralize the solution and remove excessive chlorides. Finally, iron oxide nanoparticles, in particular ~440 mg of Fe_3O_4 NPs obtained with the abovementioned procedure, were suspended in water with the desired volume. Fe_3O_4 NPs needs to be shaken vigorously before the plant application for the fast sedimentation at the bottom of the container.

Modification of Fe_3O_4 NPs with citrate

The 1 g of citric acid ($\text{C}_6\text{H}_8\text{O}_7$; CA; Warchem Sp. z o.o., Warsaw, Poland) was dissolved in 50 mL of distilled water and the 0.05 M NaOH (Warchem, Warsaw, Poland) solution was added dropwise to adjust pH 6.5. Then, the citrate solution was added to the wet obtained Fe_3O_4 NPs that were collected at the bottom of the beaker after the washing. Next, the suspension was stirred magnetically with an initial rate of 600 rpm for 10 min and then, at 200 rpm at 60 °C overnight. After that time, the suspension was stirred without heating for 1 h. When the magnetic bar was removed, the suspension was split into three Falcon-type plastic tubes and filled with acetone up to 40 mL and centrifuged for 5 min at 7000 rpm to separate $\text{Fe}_3\text{O}_4\text{CA}$ NPs from the solution containing excessive citrate. After centrifuging, the washing was repeated three times with an acetone-water mixture and last, $\text{Fe}_3\text{O}_4\text{CA}$ NPs were suspended in water. To remove acetone traces, the solution was warmed up to 50 °C for 1 h, refilled with deionized water to the desired volume and vortexed for 5 min. In contrast to Fe_3O_4 NPs, citrate-coated nanoparticles form a stable colloidal suspension in water, so no additional stirring is needed to apply on plants.

Characterization of Fe_3O_4 NPs and $\text{Fe}_3\text{O}_4\text{CA}$ NPs

The morphology of Fe_3O_4 NPs and $\text{Fe}_3\text{O}_4\text{CA}$ NPs was investigated using Scanning Electron Microscopy (SEM) - Merlin, Zeiss, Berlin, Germany and Transmission Electron

Microscopy (TEM) - Libra, Zeiss, Berlin, Germany to provide information on the size and shape of synthesized particles.

To confirm the coating of as-synthesized NPs with citrate, the FT-IR analysis was implemented using Spectrum-Two ATR – Perkin Elmer supplied by Pro-Environment, Warsaw, Poland, where the measurements were made in the range from 4000 to 450 cm^{-1} .

In addition to the FTIR studies, citrate content was estimated by the thermogravimetric analysis (TGA) using TGA 8000 – Perkin Elmer equipment supplied by Pro-Environment. Measurements were done in the nitrogen atmosphere with the purge gas flow of 40 mL min^{-1} in the temperature from 35 °C to 1000 °C with the step of 10 $^\circ\text{C} \cdot \text{min}^{-1}$.

Culture medium and physical conditions in the growth room

The MS (Murashige and Skoog 1962) medium, supplemented with 3% (w/v) sucrose and solidified with 0.8% (w/v) agar, was utilized for the initial propagation of plants. The pH was adjusted to 5.8 using 0.1 M HCl and 0.1 M NaOH after all components were added, prior to autoclaving at 105 kPa and 121 °C for 20 min. A volume of 40 mL of the medium was then poured into 350-mL glass jars, which were sealed with plastic caps. All chemical compounds were provided by Chempur, Piekary Śląskie, Poland, except for agar (Biocorp, Warsaw, Poland).

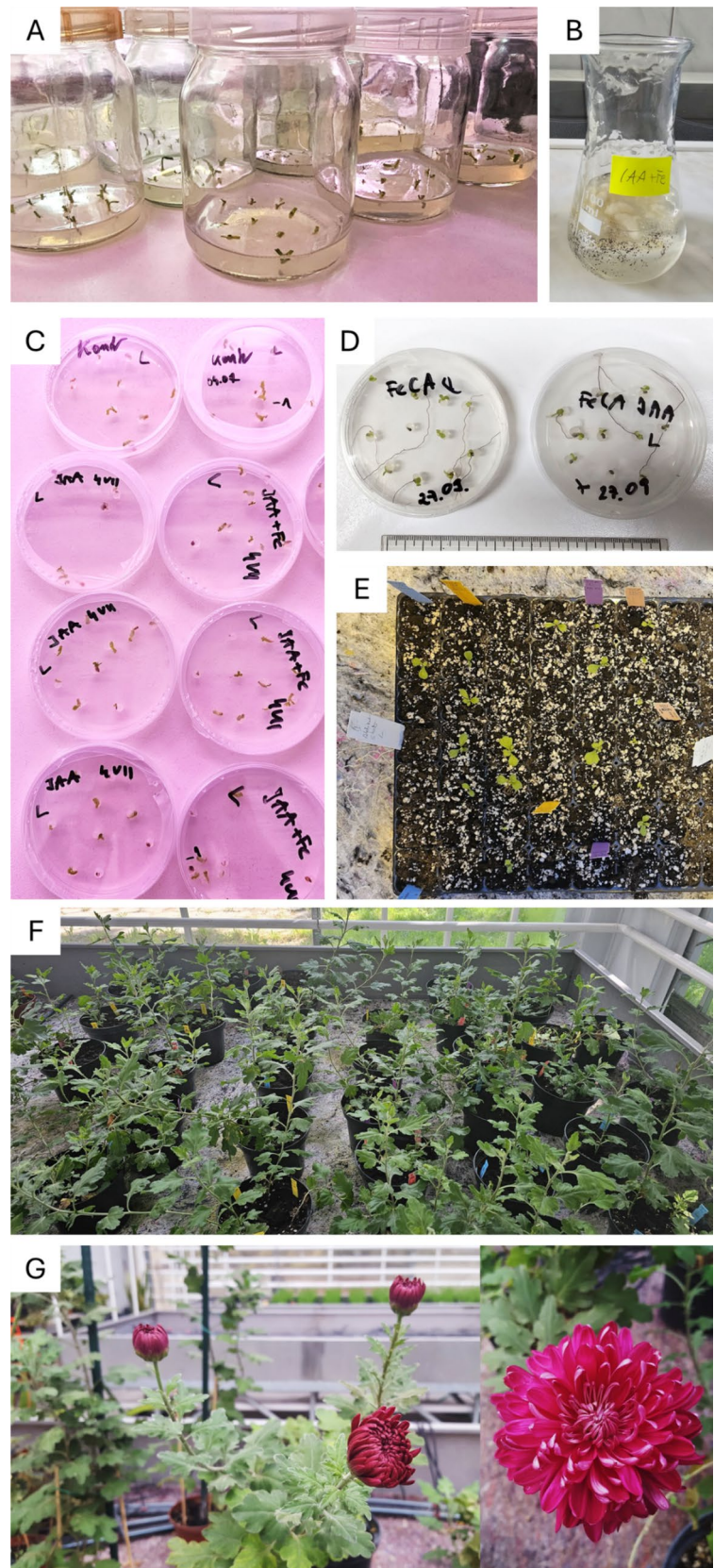
The cultures were maintained in a growth room at $24^\circ\text{C} \pm 1^\circ\text{C}$, under a 16-hour photoperiod with a photosynthetic photon flux density of approximately 30.0 $\mu\text{mol} \cdot \text{m}^{-2} \cdot \text{s}^{-1}$, provided by standard cool daylight TLD 54/36 W fluorescent lamps (Koninklijke Philips Electronics N.V., Eindhoven, The Netherlands) with a color temperature of 6200 K.

Biological material and multiplication of plants

In vitro-derived plants of chrysanthemum (*Chrysanthemum × morifolium* /Ramat./ Hemsl.) ‘Richmond’ were utilized as the source of explants. Axenic cultures were maintained in the *in vitro* gene bank of the Laboratory of Horticulture, Bydgoszcz University of Science and Technology.

The donor plants, measuring approximately 10–12 cm in length, were cloned using the single-node method in MS medium without plant growth regulators to obtain the required amount of plant material. For this purpose, shoots were segmented into nodal pieces and cultured on fresh medium (seven explants per jar) for eight weeks (Fig. 1A).

Fig. 1 Production, storage and growth of chrysanthemum ‘Richmond’ synthetic seeds. **A** – single node explants used as the source of explants (axillary buds) for the production of synthetic seeds; **B** – preparation of sodium alginate with iron nanoparticles (visible in the form of dark suspension); **C** – synthetic seeds on water-agar medium after two months of refrigeration ($+4^{\circ}\text{C}$); **D** – synthetic seeds after 30-day germination in the growth room; **E** – synthetic seeds sown into multi-pot in glasshouse; **F** – chrysanthemums grown in pots on benches; **G** – flowering plants at the beginning and full bloom



Preparation, storage and in vitro germination of synthetic seeds

Nodal segments (3–4 mm in length) with a single axillary bud were used in the experiments. Explants were excised using a micro-scalpel and binocular microscope, then immersed for 10 min in 3% (w/v) sodium alginate. The alginate solution was prepared on MS medium salts, without calcium II chloride (CaCl_2), with the addition of 3% (w/v) sucrose, iron oxide nanoparticles (pure Fe_3O_4 NPs or stabilized with citrate $\text{Fe}_3\text{O}_4\text{CA}$ NPs; $7.7 \text{ mg}\cdot\text{L}^{-1}$) and/or indole-3-acetic acid (IAA; $1 \text{ mg}\cdot\text{L}^{-1}$). IAA was obtained from Sigma-Aldrich, Darmstadt, Germany (Fig. 1B). Before beads formation, alginate solutions with NPs were placed for 30 min in the Elmasonic S80(H) Ultrasonic Cleaner (37 kHz, 150 W; Elma Schmidbauer GmbH, Singen, Germany) for proper nanoparticles dispersion. Subsequently, the beads, measuring 4–5 mm in diameter, were hardened in a 0.1 M CaCl_2 solution for 30 min. The encapsulated explants were then rinsed thrice with distilled sterile water to eliminate any excess CaCl_2 . A control group without NPs or IAA was also included. Following this, the synthetic seeds were inoculated onto a water-agar medium in a 90-mm Petri dish sealed with parafilm (10 explants per dish). Each culture dish was regarded as a single repetition. The experiment was repeated at least five times – a total of 435 shoot tips were used. The cultures were stored in a refrigerator at 4 °C in the dark for 60 days and then transferred to the initial growth room for another month (Fig. 1C). The share of germinating synthetic seeds was evaluated. The length of shoots, rooting effectiveness, and length of the longest root were measured in all plants (Fig. 1D).

Ex vitro growth and biochemical analysis of plants

The initially germinated synthetic seeds were sown in a greenhouse in January 2024, in a mixture of peat and perlite (2:1, v/v), provided by Hartmann (Poznań, Poland), in multi-pots (one seed per cell) (Fig. 1E). The acclimatization efficiency, i.e. survival of chrysanthemum plants ex vitro, was measured two weeks after transferring the plants to the greenhouse. In April, the plants were transplanted into plastic pots filled with the same substrate and grown for another three months (Fig. 1F).

The relative content of flavonoids, anthocyanins, chlorophyll content index (CCI), and Leaf Soil-Plant Analysis Development (SPAD) value in the abaxial and adaxial side of leaves was measured in each plant using an MPM-100 multi-pigment meter (Opti-Sciences Inc, Hudson, NH, USA). SPAD is an indicator of plant health and nitrogen status.

The level of stress was measured based on the maximum efficiency of photosystem II (PSII) in the leaves of all plants produced. The fluorescence kinetics of chlorophyll was measured using a portable plant stress meter OS30p+

(Opti-Sciences Inc) and then initiative fluorescence (F_0), variable fluorescence (F_v), maximum fluorescence (F_m), and their ratios (F_v/F_m and F_v/F_0) were determined and expressed in relative units.

Finally, the plants were brought to full flowering to verify the phenotype of the inflorescence (Fig. 1G). To compare the colouration of leaves and florets (adaxial and abaxial sides), the Royal Horticultural Society Colour Chart (RHSCC 1966) key was used.

Experimental design and statistical analysis

Six experimental combinations were included (alginate + IAA, alginate + Fe_3O_4 NPs, alginate + $\text{Fe}_3\text{O}_4\text{CA}$ NPs, alginate + IAA + Fe_3O_4 NPs, alginate + IAA + $\text{Fe}_3\text{O}_4\text{CA}$ NPs, alginate only /control/). The experiment was performed in a completely randomized design.

The obtained results underwent statistical analysis through one-way ANOVA, and mean comparisons were conducted using Duncan's Test ($p \leq 0.05$) with Statistica 12.0 (StatSoft, Poland). As for the data based on counts expressed as percentages, with a binominal distribution, the arcsine transformation was used.

Results

Characterization of Fe_3O_4 and citrate-coated Fe_3O_4 NPs

SEM and TEM images presented in Fig. 2A-B show that Fe_3O_4 NPs and $\text{Fe}_3\text{O}_4\text{CA}$ NPs were spherical in shape with a diameter below 10 nm average. For $\text{Fe}_3\text{O}_4\text{CA}$ NPs, a tiny coat of citrate on the surface was seen (Fig. 2B).

Figure 2C shows that the FT-IR spectra for samples before and after coating differed. The sharp peak located at 552 cm^{-1} is characteristic of the vibration of Fe-O in the iron oxide-based nanoparticles and was clearly seen in both samples as expected. For the sample coated with citrate, additional peaks in the region from ~ 1000 to 3000 cm^{-1} appeared. The appearance of carboxylate-related peaks confirms the chemisorption of citrate ions onto the Fe_3O_4 surface.

Figure 2D, obtained from TGA analysis, shows major weight loss below 120 °C and the following relatively high weight loss in the higher temperature range up to 500 °C for uncoated and citrate-coated Fe_3O_4 nanoparticles. The estimated citrate content of $\text{Fe}_3\text{O}_4\text{CA}$ NPs, based on the thermograms, was approximately 6 wt%, comparing the mass loss of both samples in the temperature range above water evaporation.

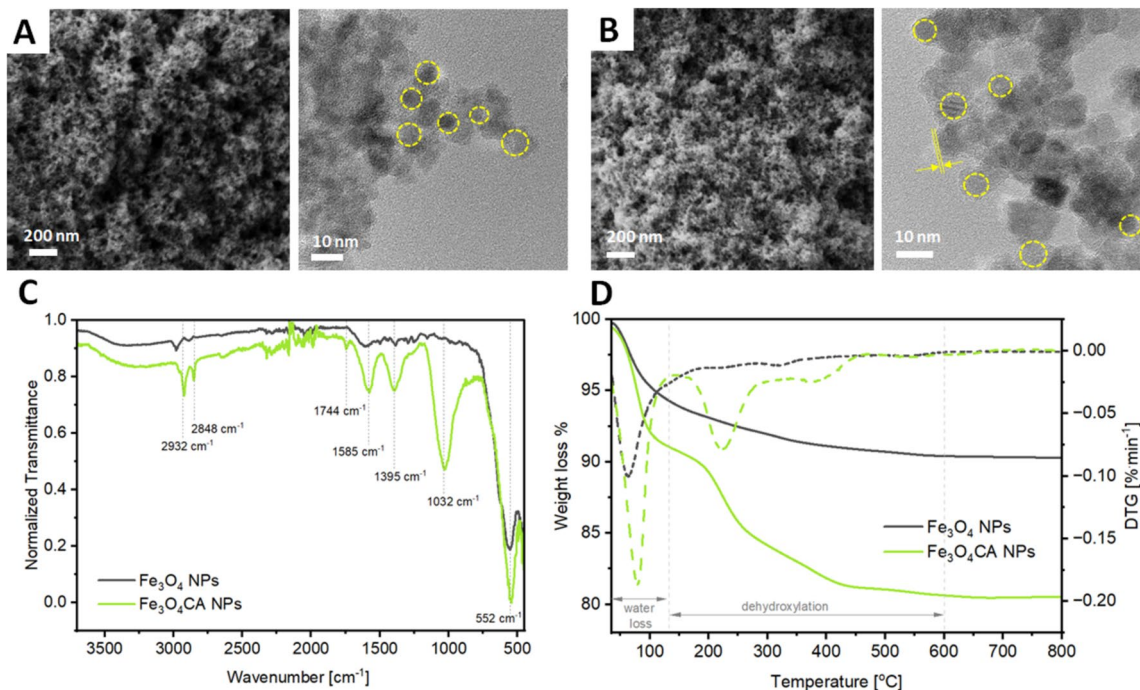


Fig. 2 SEM and TEM images of Fe_3O_4 NPs (A) and $\text{Fe}_3\text{O}_4\text{CA}$ NPs (B), FTIR spectra (C) and thermograms (D) for Fe_3O_4 NPs and $\text{Fe}_3\text{O}_4\text{CA}$ NPs

Effect of iron oxide nanoparticles and IAA on the germination and development of chrysanthemum synthetic seeds

Supplementation of alginate matrix of the synthetic seed with iron nanoparticles stabilized with citrate ($\text{Fe}_3\text{O}_4\text{CA}$ NPs), with or without the addition of IAA, enhanced the germination efficiency of cold-stored synthetic seeds of chrysanthemum 'Richmond' by over 30% compared with the control (alginate without NPs or IAA) (Fig. 3A). Likewise, the presence of these compounds stimulated the elongation of chrysanthemum shoots (6.6–6.8 mm) compared to all other treatments and the control (4.3–4.8 mm) (Fig. 3B). On the other hand, there was no effect of nanoparticles or IAA on the rooting efficiency (35–59%) (Fig. 3C). A tendency suggesting a positive impact of IAA and/or Fe_3O_4 NPs on the number of roots produced was observed, however, it was not statistically proven (Fig. 3D). IAA stimulated the elongation of roots that were nearly three-fold longer than the control (Fig. 3E). The highest acclimatization efficiency (63%) was found when adding both IAA and $\text{Fe}_3\text{O}_4\text{CA}$ NPs into the alginate beads. The presence of $\text{Fe}_3\text{O}_4\text{CA}$ NPs alone also provided a high survival level (42%) of ex vitro-grown plants that was significantly different from the control (19%) (Fig. 3F).

Effect of iron oxide nanoparticles and IAA on the physiological activity of chrysanthemum plants

It was found that the presence of Fe_3O_4 NPs in the synthetic seed increased the relative content of flavonoids in the adaxial side of chrysanthemum leaves (0.75) compared with the control (0.53) (Table 1). No differences between the control and IAA- and/or NPs-treated plants was reported in terms of flavonoid level in the abaxial side of leaves, but the plants treated with Fe_3O_4 NPs contained significantly more pigments (0.74) than those treated with $\text{Fe}_3\text{O}_4\text{CA}$ NPs (0.45). Difference in anthocyanins content was observed only in the abaxial side of leaves between plants treated with Fe_3O_4 NPs (0.021) and the control (0.032). No effect of NPs or IAA on the concentration of chlorophyll or SPAD value in both abaxial or adaxial side of leaves was found (Table 1).

The addition of Fe_3O_4 NPs into the synthetic seed decreased the chlorophyll fluorescence parameters (F_0 , F_v , and F_m), while the combination of IAA and $\text{Fe}_3\text{O}_4\text{CA}$ NPs increased the initiative fluorescence (F_0) as compared with the control (Table 2). The F_v/F_m and F_v/F_0 values remained unchanged in most experimental treatments, except for the combination IAA + $\text{Fe}_3\text{O}_4\text{CA}$ NPs, in which they were significantly lower (0.815 and 4.43, respectively) than in the control (0.823 and 4.67) (Table 2).

Flowering plants of chrysanthemum from all experimental treatments were identified with the same RHSCC code

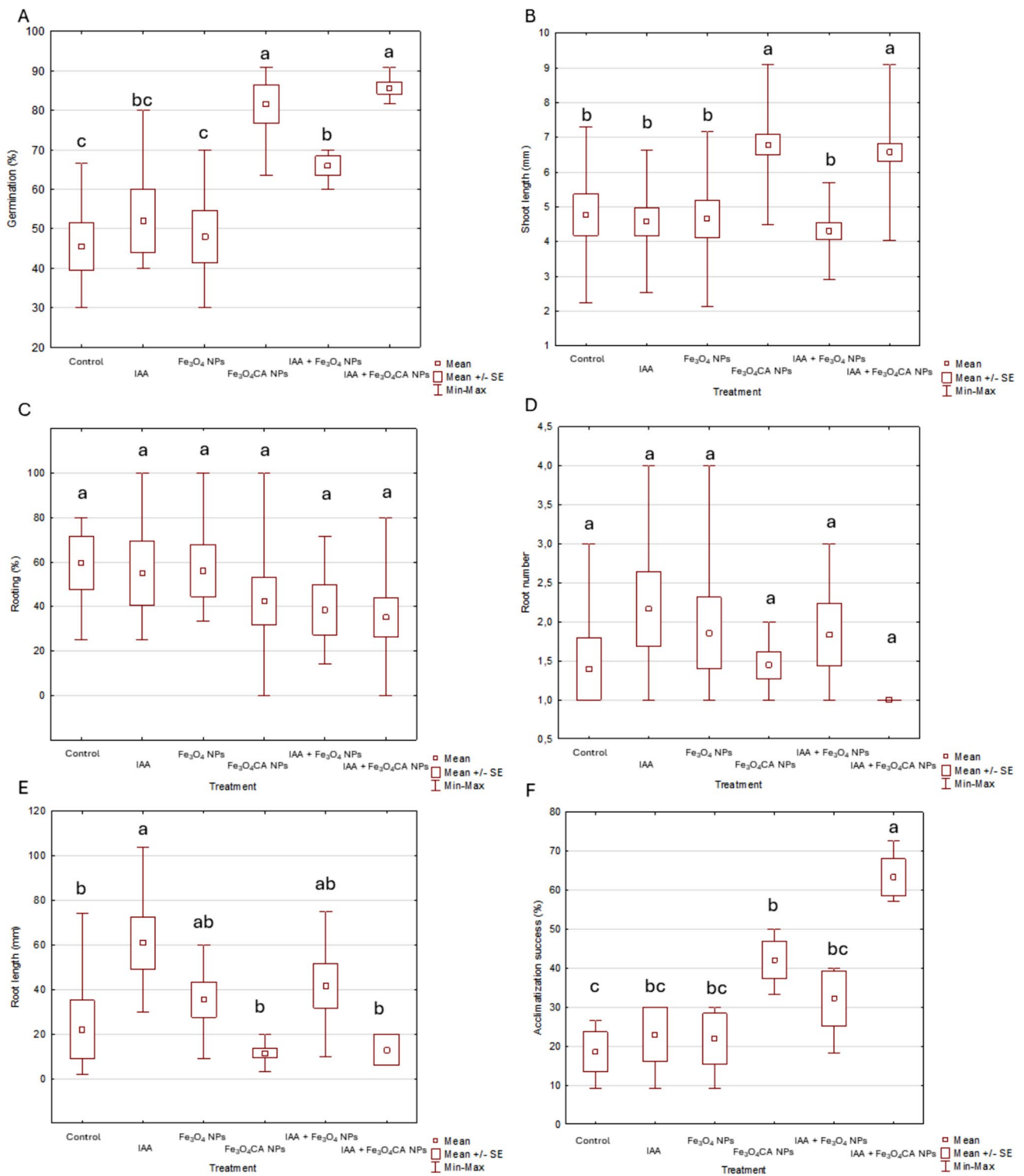


Fig. 3 Effect of indole-3-acetic acid (IAA) and iron nanoparticles in pure (Fe₃O₄ NPs) or stabilized form (Fe₃O₄CA NPs), applied singularly or in combination, on the germination efficiency of synthetic seeds (A), shoot length (B), rooting efficiency (C), root number per

shoot (D), length of the longest root and acclimatization efficiency of chrysanthemum ‘Richmond’. Means ± standard errors (SE) that share the same letter do not differ significantly according to Duncan’s test at $p \leq 0.05$

Table 1 Effect of indole-3-acetic acid (IAA) and iron nanoparticles in pure (Fe₃O₄ NPs) or stabilized form (Fe₃O₄CA NPs), applied singularly or in combination, on the relative content of flavonoids, antho-

cyanins, chlorophyll (CCI) and SPAD value in the adaxial and abaxial sides of chrysanthemum 'Richmond' leaves

Treatment	Flavonoids		Anthocyanins		CCI		SPAD	
	Adaxial	Abaxial	Adaxial	Abaxial	Adaxial	Abaxial	Adaxial	Abaxial
Control	0.53 ± 0.05 bc	0.54 ± 0.05 abc	0.033 ± 0.004 a	0.032 ± 0.003 a	20.4 ± 1.6 a	20.4 ± 1.6 a	43.8 ± 1.4 a	43.8 ± 1.4 a
IAA	0.71 ± 0.10 ab	0.72 ± 0.10 ab	0.027 ± 0.003 a	0.027 ± 0.003 ab	17.4 ± 1.3 a	17.4 ± 1.3 a	41.2 ± 1.2 a	41.2 ± 1.2 a
Fe ₃ O ₄ NPs	0.75 ± 0.08 a	0.74 ± 0.08 a	0.027 ± 0.003 a	0.027 ± 0.003 ab	18.8 ± 1.5 a	18.8 ± 1.5 a	42.6 ± 1.3 a	42.6 ± 1.3 a
Fe ₃ O ₄ CA NPs	0.51 ± 0.06 bc	0.45 ± 0.02 c	0.026 ± 0.003 a	0.021 ± 0.002 b	16.7 ± 1.2 a	15.8 ± 0.8 a	40.5 ± 1.2 a	39.4 ± 0.8 a
IAA + Fe ₃ O ₄ NPs	0.63 ± 0.05 abc	0.52 ± 0.06 bc	0.031 ± 0.002 a	0.024 ± 0.002 ab	18.9 ± 1.4 a	16.6 ± 1.2 a	42.0 ± 0.9 a	40.4 ± 1.2 a
IAA + Fe ₃ O ₄ CA NPs	0.44 ± 0.04 c	0.64 ± 0.05 abc	0.038 ± 0.014 a	0.029 ± 0.002 ab	16.1 ± 0.8 a	18.0 ± 0.9 a	39.7 ± 0.8 a	41.6 ± 0.8 a

Means in columns (± standard errors) that share the same letter do not differ significantly according to Duncan's test at $p \leq 0.05$

for the adaxial and abaxial sides of leaves (137B/138B, respectively) and florets (61B/62B). All inflorescences were of purple colour (Fig. 1G).

Discussion

The present study highlights the promising application of indole-3-acetic acid (IAA) and iron oxide nanoparticles (Fe₃O₄ NPs) in enhancing the germination and growth of synthetic seeds of chrysanthemum (*Chrysanthemum × morifolium* 'Richmond'). These findings are particularly relevant given the importance of chrysanthemum as a high-value ornamental species with considerable commercial and horticultural significance (Miler and Woźny, 2021).

Physicochemical properties of NPs

The results indicate that the synthesis method proposed here improved the overall process, resulting in smaller nanoparticles (diameter below 10 nm average) that are more favorable to plant uptake. The nanoparticles synthesized with the co-precipitation method in similar conditions but excluding the addition of HCl resulted in a higher diameter of samples

about ~ 15 nm average (Osial et al. 2022; Pietrzyk et al. 2022). It has been previously reported that smaller NPs are more easily absorbed and transported within the symplast and apoplast (Sembada and Lenggono 2024), which could explain the high efficiency of NPs in the current study.

FT-IR analysis confirmed that citrate was effectively bonded to the surface of the Fe₃O₄ NPs, where new peaks in the citrate-coated sample appeared comparing to the non-coated NPs. The peaks at 1032 cm⁻¹ and 1395 cm⁻¹ can be assigned to the C–O stretching (Wang et al. 2003; Jeong et al. 2013). The following peak at 1585 cm⁻¹ can relate to the O–H stretching in the carboxylic groups at citrate (Osial et al., 2024). The peak observed at 1744 cm⁻¹ can be assigned to the C=O stretching in carboxylates (Talelli et al. 2009), while the appearance of peaks at 2848 cm⁻¹ and 2932 cm⁻¹ can be ascribed to alkyl chain –CH₂ symmetric and asymmetric stretching in the citrate structure, respectively (Nwaji et al. 2017; Wierzbinski et al., 2018). The presence of the citrate coating on the Fe₃O₄ NPs suggests enhanced functionalization that may influence the interaction of these NPs with biological systems.

The significant weight loss observed in the TGA analysis further supports the claims on successful coating of nanoparticles with citrate, indicating that the modification effectively alters their thermal stability and possibly their bioavailability. The major weight loss for both CA-coated

Table 2 Effect of indole-3-acetic acid (IAA) and iron nanoparticles in pure (Fe₃O₄ NPs) or stabilized form (Fe₃O₄CA NPs), applied singularly or in combination, on the chlorophyll fluorescence parameters and ratios of chrysanthemum 'Richmond' leaves

Treatment	F _o	F _v	F _m	F _v /F _m	F _v /F _o
Control	151.8 ± 2.9 b	706.8 ± 9.0 a	858.6 ± 10.7 ab	0.823 ± 0.003 a	4.67 ± 0.08 a
IAA	154.8 ± 1.4 ab	712.4 ± 7.9 a	867.2 ± 8.7 a	0.821 ± 0.002 ab	4.60 ± 0.05 ab
Fe ₃ O ₄ NPs	142.8 ± 2.9 c	657.9 ± 12.8 c	800.8 ± 15.4 c	0.821 ± 0.002 ab	4.61 ± 0.05 ab
Fe ₃ O ₄ CA NPs	154.2 ± 1.2 ab	710.1 ± 5.4 a	864.4 ± 6.2 a	0.821 ± 0.001 ab	4.61 ± 0.03 ab
IAA + Fe ₃ O ₄ NPs	150.1 ± 1.7 b	682.9 ± 7.8 b	833.1 ± 8.8 b	0.819 ± 0.002 ab	4.55 ± 0.05 ab
IAA + Fe ₃ O ₄ CA NPs	159.0 ± 2.1 a	700.5 ± 3.8 ab	859.5 ± 4.7 ab	0.815 ± 0.002 b	4.43 ± 0.05 b

Means in columns (± standard errors) that share the same letter do not differ significantly according to Duncan's test at $p \leq 0.05$

and non-coated samples below 120 °C corresponds to the evaporation of the water that was physically adsorbed onto the surface of nanoparticles (Noqta et al. 2020). The following relatively high weight loss in the higher temperature range up to 500 °C comes from the dehydroxylation (Karami et al. 2020).

Germination and growth of chrysanthemum plants

Incorporation of IAA (1.0 mg·L⁻¹) and Fe₃O₄ NPs (7.7 mg·L⁻¹), particularly when stabilized with citrate (Fe₃O₄CA NPs), in the alginate matrix of synthetic seeds substantially improved germination efficiency compared to the control group. This enhancement in germination rates is crucial for commercial applications where synthetic seed technology's high efficiency and reliability are paramount (Gantait et al. 2015). In contrast, Fe₂O₃ NPs had no significant effect on *Kobresia capillifolia* (Decne.) C.B. Clarke seed germination (Sun et al. 2023). This can be attributed to the fact that plant responses to iron nanoparticles differ among species, NPs characteristics, and environmental conditions (Lead et al. 2018). Moreover, here we used Fe₃O₄ NPs, which in contrast to more often studied Fe₂O₃ NPs, contain Fe in both +2 and +3 oxidation states, and are therefore more versatile.

In the present study, the elongation of chrysanthemum shoots was significantly stimulated by the presence of NPs and auxin, with treated shoots exhibiting lengths approximately 37% greater than those of the control. This suggests that IAA and Fe₃O₄CA NPs not only facilitate the initial germination but also promote subsequent vegetative growth, potentially leading to more robust and viable plants. Likewise, titanium dioxide nanoparticles (TiO₂ NPs) stimulated the elongation of wheat (*Triticum aestivum* L.) seedlings, but only at low concentrations (up to 10 mg·L⁻¹). Higher levels of nanoparticles had an inhibitory effect (Jaberzadeh et al. 2013). It would be interesting in future to study other concentrations of iron nanoparticles, to fully understand their impact on plants.

The present study found no significant impact of IAA and NPs treatments on the rooting efficiency, with percentages ranging between 35% and 59% across all experimental conditions. This indicates that while Fe₃O₄CA NPs enhance shoot development, their effect on root initiation is limited. Nonetheless, there was a notable, albeit not statistically significant, trend suggesting that these treatments might increase the number of roots produced. This is a considerable step forward, as according to Tymoszuk and Miler (2019), chrysanthemum leaf explants ('Bydgoszczanka') treated with 10 and 30 mg·L⁻¹ silver nanoparticles (Ag NPs) produced less adventitious roots compared to the control group. In the present study, IAA treatment alone resulted in roots that were nearly three times longer than those in the control, underscoring the role of IAA in promoting root

elongation, which has also been observed in other crops (Abu-Zahra et al. 2013).

The highest acclimatization efficiency (63%) was observed in the treatment combining IAA and Fe₃O₄CA NPs, which is a critical factor for the successful establishment of plants *ex vitro* (Jagiello-Kubiec et al. 2021). The significant survival rate of plants treated with Fe₃O₄CA NPs alone (42%) compared to the control (19%) further highlights the potential of these nanoparticles in improving the *ex vitro* performance of synthetic seeds.

Physiological activity

The physiological assessments of chrysanthemum plants revealed that Fe₃O₄ NPs contributed to an increased relative content of flavonoids in the adaxial side of the leaves. This enhancement in flavonoid content could be indicative of improved stress resistance and overall plant health, given the role of flavonoids in plant defence mechanisms (Dias et al. 2021). This hypothesis is supported by the decreased initial fluorescence value (F₀). However, the study did not observe significant differences in flavonoid levels on the abaxial side of the leaves across NPs treatments and the control, suggesting a differential distribution or regulation of these compounds within the leaf tissue. The complex aspects of nanoparticle transport and their accumulation within plant organs were described Pérez-de-Luque (2017). It is possible that in chrysanthemum, trichomes present in the adaxial side of leaves were involved in the internal immobilization of NPs, as observed in pine (*Pinus sylvestris* L.) and beech (*Fagus sylvatica* L.) (Ballikaya et al. 2023). This should be considered when applying nanoparticles in the form of foliar spray.

Interestingly, the presence of Fe₃O₄ NPs alone led to a higher flavonoid content in both leaf surfaces compared to Fe₃O₄CA NPs, highlighting potential variations in the biochemical impact of different nanoparticle forms. Absorption spectra of flavonoids are strongly pH-dependent. Cellular pH plays an essential role in pigment content, which could explain why the results for nanoparticles stabilized with citrate (CA) were different from those without it (Stavenga et al. 2021). Conversely, the anthocyanin content was lower in plants treated with Fe₃O₄ NPs compared to the control, suggesting that the nanoparticles might influence the biosynthesis or accumulation of specific pigments differently, which is in agreement with the findings of Kruszka et al. (2020; 2022). Metabolomics studies indicate that NPs affect the levels of secondary metabolites in plants by modulating reactive nitrogen and oxygen species, as well as gene expression and signalling pathways, all of which could contribute to our results (Selvakesavan et al. 2023).

The chlorophyll fluorescence parameters, which are indicative of the photosynthetic efficiency and stress status

of the plants, were variably affected by the treatments. The addition of Fe_3O_4 NPs resulted in decreased fluorescence parameters (F_0 , F_v , and F_m), while the combination of IAA and $\text{Fe}_3\text{O}_4\text{CA}$ NPs increased the initial fluorescence (F_0). F_m is the maximum fluorescence level achieved when all PSII reaction centres are closed. A decrease in F_m suggests a reduction in the plant's capacity to reduce all PSII reaction centres (Sharma et al. 2014). On the other hand, F_0 represents the minimum fluorescence level when all photosystem II (PSII) reaction centres are open in a dark-adapted state (Zhang et al. 2022). An increase in F_0 accompanied by a decrease in F_v/F_0 observed in the treatment IAA + $\text{Fe}_3\text{O}_4\text{CA}$ NPs (4.43 vs. 4.67 in the control) indicates stress-induced damage to PSII reaction centres or impaired energy transfer from light-harvesting complexes to reaction centres that slightly affected the plant's photosynthetic apparatus (Kalaji et al. 2012). Nonetheless, according to Maxwell and Johnson (2000), in healthy plants, the F_v/F_m value typically ranges from 0.79 to 0.84. The obtained here values (from 0.815 to 0.823) indicate the overall good health quality status of all plants.

In summary, the integration of nanotechnology and plant growth regulators holds significant promise for advancing synthetic seed technology and enhancing the productivity and quality of ornamental perennials such as chrysanthemum. Citrate-stabilized nanoparticles were overall more effective than traditional Fe_3O_4 NPs. Likewise, Iannone et al. (2021) reported no phytotoxic effect and stimulatory activity of magnetite nanoparticles coated with CA on the growth of alfalfa (*Medicago sativa* L.) and soybean (*Glycine max* L.). Surface coverage with citrate provides a more thermodynamically stable colloidal solution, leaving additional carboxyl groups on the nanoparticle surface and simultaneously preventing their aggregation (Mikelashvili et al. 2023), which could explain the obtained here better results. Since citric acid shows bactericidal and bacteriostatic effects and solutions containing CA are utilized as sterilizing agents (Khan et al. 2020), in addition to the bacteriostatic properties of Fe, further research could focus on the direct ex vitro sowing of $\text{Fe}_3\text{O}_4\text{CA}$ NPs-fortified synthetic seeds directly into the soil.

Conclusions

The results of this study demonstrate the significant beneficial effect of incorporating iron oxide nanoparticles stabilized with citrate ($\text{Fe}_3\text{O}_4\text{CA}$ NPs) and indole-3-acetic acid (IAA) in the production and storage of chrysanthemum synthetic seeds. The combination of these additives markedly enhanced germination efficiency, reaching 86% compared to 47% in the control. $\text{Fe}_3\text{O}_4\text{CA}$, both with and without IAA, promoted shoot elongation, while IAA stimulated

root elongation, indicating complementary roles in plant development. The simultaneous application of IAA and $\text{Fe}_3\text{O}_4\text{CA}$ NPs in the alginate coating improved acclimatization efficiency, increasing survival rates from 19% in the control to 63%. The influence of iron oxide nanoparticles on the secondary metabolite profile was observed, though chlorophyll content remained unchanged, which opens new areas of research on the elicitation of metabolites production. Chlorophyll fluorescence measurements confirmed the overall good health and photosynthetic efficiency of the plants, despite some stress induced by nanoparticle exposure. Importantly, the phenotypic uniformity of the plants derived from synthetic seeds was maintained. The successful storage of synthetic seeds at 4 °C for 60 days indicates the potential for medium-term preservation of chrysanthemum germplasm. Our research also contributes to better understanding the physicochemical properties of Fe_3O_4 and citrate-coated Fe_3O_4 NPs. These findings have significant implications for improving propagation techniques in horticulture and plant biotechnology, particularly for chrysanthemum and potentially other ornamental species with high levels of self-incompatibility and heterozygosity. Future research will aim to use other nanoparticle types and study their interaction with various classes of plant growth regulator.

Supplementary Information The online version contains supplementary material available at <https://doi.org/10.1007/s11240-024-02955-7>.

Acknowledgements The authors wish to thank Aleksandra Piszczek for her technical support in performing the experiment.

Funding This research received no external funding.

Data availability Data available by email on reasonable request.

Declarations

Competing interests The authors have no relevant financial or non-financial interests to disclose.

References

- Abu-Zahra TR, Al-Shadaideh AN, Abubaker SM, Qrunfleh IM (2013) Influence of auxin concentrations on different ornamental plants rooting. *Int J Bot* 9:96–99. <https://doi.org/10.3923/ijb.2013.96.99>
- Ahmed MA, Shafiei-Masouleh S-S, Mohsin RM, Salih ZK (2023) Foliar application of iron oxide nanoparticles promotes growth, mineral contents, and medicinal qualities of *Solidago Virgaurea* L. *J. Soil Sci. Plant Nutr* 23:2610–2624. <https://doi.org/10.1007/s42729-023-01218-2>
- Ballikaya P, Brunner I, Coccozza C, Grolimund D, Kaegi R, Murazzi ME, Schaub M, Schönbeck LC, Sinnet B, Cherubini P (2023) First evidence of nanoparticle uptake through leaves and roots in beech (*Fagus sylvatica* L.) and pine (*Pinus sylvestris* L.). *Tree Physiol* 43(2):262–276. <https://doi.org/10.1093/treephys/tpac117>


- Dias MC, Pinto DCGA, Silva AMS (2021) Plant flavonoids: chemical characteristics and biological activity. *Molecules* 26(17):5377. <https://doi.org/10.3390/molecules26175377>
- El-Desouky HS, Islam KR, Bergefurd B, Gao G, Harker T, Abd-El-Dayem H, Ismail F, Mady M, Zewail RMY (2021) Nano iron fertilization significantly increases tomato yield by increasing plants' vegetable growth and photosynthetic efficiency. *J Plant Nutr* 44(11):1649–1663. <https://doi.org/10.1080/01904167.2021.1871749>
- Feng Y, Kreslavski VD, Shmarev AN, Ivanov AA, Zharmukhamedov SK, Kosobryukhov A, Yu M, Allakhverdiev SI, Shabala S (2022) Effects of iron oxide nanoparticles (Fe₃O₄) on growth, photosynthesis, antioxidant activity and distribution of mineral elements in wheat (*Triticum aestivum*) plants. *Plants* 11:1894. <https://doi.org/10.3390/plants11141894>
- Fraceto LF, Grillo R, de Medeiros GA, Scognamiglio V, Rea G, Bartolucci C (2016) Nanotechnology in agriculture: which innovation potential does it have? *Front Environ Sci* 4:20. <https://doi.org/10.3389/fenvs.2016.00020>
- Gantait S, Kundu S, Ali N, Sahu NC (2015) Synthetic seed production of medicinal plants: a review on influence of explants, encapsulation agent and matrix. *Acta Physiol Plant* 37:98. <https://doi.org/10.1007/s11738-015-1847-2>
- Iannone MF, Groppa MD, Zawoznik MS, Coral DF, Fernández van Raap MB, Benavides MP (2021) Magnetite nanoparticles coated with citric acid are not phytotoxic and stimulate soybean and alfalfa growth. *Ecotoxicol Environ Saf* 211:111942. <https://doi.org/10.1016/j.ecoenv.2021.111942>
- Jaberzadeh A, Moaveni P, Moghadam T, Zahedi HR, H (2013) Influence of bulk and nanoparticles titanium foliar application on some agronomic traits, seed gluten and starch contents of wheat subjected to water deficit stress. *Not Bot Horti Agrobo* 41(1):201–207. <https://doi.org/10.15835/nbha4119093>
- Jagiello-Kubiec K, Nowakowska K, Łukaszewska AJ, Pacholczak A (2021) Acclimation to *ex vitro* conditions in ninebark. *Agronomy* 11:612. <https://doi.org/10.3390/agronomy11040612>
- Jeong HS, Venkatesan J, Kim SK (2013) Isolation and characterization of collagen from marine fish (*Thunnus obesus*). *Biotechnol Bioproc Eng* 18:1185–1191. <https://doi.org/10.1007/s12257-013-0316-2>
- Jerzy M, Zalewska M, Tymoszek A (2015) Effect of kinetin on the elongation of adventitious shoots regenerated *in vitro* from ligulate florets in *Chrysanthemum* × *Grandiflorum* Ramat. *Acta Hort* 1083:577–584. <https://doi.org/10.17660/ActaHortic.2015.1083.77>
- Jin M, Liu Y, Shi B, Yuan H (2023) Exogenous IAA improves the seedling growth of *Syringa villosa* via regulating the endogenous hormones and enhancing the photosynthesis. *Sci Hortic* 308:111585. <https://doi.org/10.1016/j.scienta.2022.111585>
- Kalaji HM, Carpentier R, Allakhverdiev SI, Bosa K (2012) Fluorescence parameters as early indicators of light stress in barley. *J Photochem Photobiol B: Biol* 112:1–6. <https://doi.org/10.1016/j.jphotobiol.2012.03.009>
- Karakeçili A, Korpayev S, Dumanoglu H, Alizadeh S (2019) Synthesis of indole-3-acetic acid and indole-3-butyric acid loaded zinc oxide nanoparticles: effects on rhizogenesis. *J Biotechnol* 303:8–15. <https://doi.org/10.1016/j.jbiotec.2019.07.004>
- Karami Z, Ganjali MR, Zarghami Dehaghani M, Aghazadeh M, Jouyandeh M, Esmaeili A, Habibzadeh S, Mohaddespour A, Formela I, Haponiu K, Saeb JT (2020) Kinetics of cross-linking reaction of epoxy resin with hydroxyapatite-Functionalized layered double hydroxides. *Polymers* 12:1157. <https://doi.org/10.3390/polym12051157>
- Kasote DM, Lee JHJ, Jayaprakasha GK, Patil BS (2019) Seed priming with iron oxide nanoparticles modulate antioxidant potential and defense-linked hormones in watermelon seedlings. *ACS Sustain Chem Eng* 7(5):5142–5151. <https://doi.org/10.1021/acssuschemeng.8b06013>
- Khan S, Shah ZH, Riaz S, Ahmad N, Islam S, Raza MA, Naseem S (2020) Antimicrobial activity of citric acid functionalized iron oxide nanoparticles –superparamagnetic effect. *Ceram Internat* 46(8):10942–10951. <https://doi.org/10.1016/j.ceramint.2020.01.109>
- Kruszka D, Sawikowska A, Kamalabai Selvakesavan R, Krajewski P, Kachlicki P, Franklin G (2020) Silver nanoparticles affect phenolic and phytoalexin composition of *Arabidopsis thaliana*. *Sci Total Environ* 716:135361. <https://doi.org/10.1016/j.scitotenv.2019.135361>
- Kruszka D, Selvakesavan RK, Kachlicki P, Franklin G (2022) Untargeted metabolomics analysis reveals the elicitation of important secondary metabolites upon treatment with various metal and metal oxide nanoparticles in *Hypericum perforatum* L. cell suspension cultures. *Ind Crops Prod* 178:114561. <https://doi.org/10.1016/j.indcrop.2022.114561>
- Kulus D, Zalewska M (2014) In vitro plant recovery from alginate encapsulated *Chrysanthemum* × *grandiflorum* /Ramat./ kitam. Shoot tips. *Prop Ornament Plants* 14(1):3–12
- Lead JR, Batley GE, Alvarez PJJ, Croteau MN, Handy RD, McLaughlin MJ, Judy JD, Schirmer K (2018) Nanomaterials in the environment: behavior, fate, bioavailability, and effects—an updated review. *Environ Toxicol Chem* 37(8):2029–2063. <https://doi.org/10.1002/etc.4147>
- Li P, Wang A, Du W, Mao L, Wei Z, Wang S, Yuan H, Ji R, Zhao L (2020) Insight into the interaction between Fe-based nanomaterials and maize (*Zea mays*) plants at metabolic level. *Sci Total Environ* 738:139795. <https://doi.org/10.1016/j.scitotenv.2020.139795>
- Maswada HF, Djanaguiraman M, Prasad PVV (2018) Seed treatment with nano-iron (III) oxide enhances germination, seedling growth and salinity tolerance of sorghum. *J Agro Crop Sci* 204:577–587. <https://doi.org/10.1111/jac.12280>
- Maxwell K, Johnson GN (2000) Chlorophyll fluorescence – a practical guide. *J Exp Bot* 51(345):659–668. <https://doi.org/10.1093/jxb/51.345.659>
- Mikelashvili V, Kekutia S, Markhulia J, Saneblidze L, Maisuradze N, Kriechbaum M, Almásy L (2023) Synthesis and characterization of citric acid-modified iron oxide nanoparticles prepared with electrohydraulic discharge treatment. *Materials* 16:746. <https://doi.org/10.3390/ma16020746>
- Miler N, Wozny A (2021) Effect of pollen genotype, temperature and period of storage on *in vitro* germinability and *in vivo* seed set in chrysanthemum – preliminary study. *Agronomy* 11:2395. <https://doi.org/10.3390/agronomy11122395>
- Murashige T, Skoog F (1962) A revised medium for rapid growth and bio assays with tobacco tissue cultures. *Physiol Plant* 15:473–497. <https://doi.org/10.1111/j.1399-3054.1962.tb08052.x>
- Noqta OA, Sodipo BK, Aziz AA (2020) One-pot synthesis of highly magnetic and stable citrate coated superparamagnetic iron oxide nanoparticles by modified coprecipitation method. *Funct Compos Struct* 2:045005. <https://doi.org/10.1088/2631-6331/abcdbc>
- Nwaji N, Mack J, Britton J, Nyokong T (2017) Synthesis, photophysical and nonlinear optical properties of a series of ball-type phthalocyanines in solution and thin films. *New J Chem* 41:1–15. <https://doi.org/10.1039/C6NJ03662G>
- Osial M, Nowicki M, Klejman E, Fraś L (2022) Investigation of the well-dispersed magnetorheological oil-based suspension with superparamagnetic nanoparticles using modified split Hopkinson pressure bar. *Rheol Acta* 61:111–122. <https://doi.org/10.1007/s00397-021-01318-9>
- Osial M, Ha GN, Vu VH, Nguyen TP, Nieciecka D, Pietrzyk-Thel P, Urbanek O, Olusegun SJ, Wilczewski S, Giersig M, Do HT, Thanh TMD (2024) One-pot synthesis of magnetic hydroxyapatite (SPION/HAp) for 5-fluorouracil delivery and magnetic hyperthermia. *J Nanopart Res* 26:7. <https://doi.org/10.1007/s11051-023-05916-x>

- Pérez-de-Luque A (2017) Interaction of nanomaterials with plants: what do we need for real applications in agriculture? *Front. Environ Sci* 5:12. <https://doi.org/10.3389/fenvs.2017.00012>
- Pietrzyk P, Phuong NT, Olusegun SJ, Hong Nam N, Thanh DTM, Giersig M, Krysiński P, Osial M (2022) Titan Yellow and Congo Red removal with Superparamagnetic Iron-Oxide-based nanoparticles doped with zinc. *Magnetochemistry* 8(91):1–23. <https://doi.org/10.3390/magnetochemistry8080091>
- RHSCC (1966) The Royal Horticultural Society Colour Chart, London
- Selvakesavan RK, Kruska D, Shakya P, Mondal D, Franklin G (2023) Impact of nanomaterials on plant secondary metabolism. In: Al-Khayri JM, Alnaddaf LM, Jain SM (eds) *Nanomaterial interactions with plant cellular mechanisms and macromolecules and agricultural implications*. Springer, Cham, pp 133–170. https://doi.org/10.1007/978-3-031-20878-2_6
- Sembada AA, Lenggono IW (2024) Transport of nanoparticles into plants and their detection methods. *Nanomat* 14:131. <https://doi.org/10.3390/nano14020131>
- Sharma DK, Fernández JO, Rosenqvist E, Ottosen C-O, Andersen SB (2014) Genotypic response of detached leaves versus intact plants for chlorophyll fluorescence parameters under high temperature stress in wheat. *J Plant Physiol* 171(8):576–586. <https://doi.org/10.1016/j.jplph.2013.09.025>
- Stavenga DG, Leertouwer HL, Dudek B, van der Kooij CJ (2021) Coloration of flowers by flavonoids and consequences of pH dependent absorption. *Front Plant Sci* 11:600124. <https://doi.org/10.3389/fpls.2020.600124>
- Sundaria N, Singh M, Upreti P, Chauhan RP, Jaiswal JP, Kumar A (2019) Seed priming with iron oxide nanoparticles triggers iron acquisition and biofortification in wheat (*Triticum aestivum* L.) grains. *J Plant Growth Regul* 38(1):122–131. <https://doi.org/10.1007/s00344-018-9818-7>
- Sun Y, Ma L, Ma J, Li B, Zhu Y, Chen F (2022) Combined application of plant growth-promoting bacteria and iron oxide nanoparticles ameliorates the toxic effects of arsenic in Ajwain (*Trachyspermum ammi* L.). *Front. Plant Sci* 13:1098755. <https://doi.org/10.3389/fpls.2022.1098755>
- Sun H, Qu G, Li S, Song K, Zhao D, Li X, Yang P, He X, Hu T (2023) Iron nanoparticles induced the growth and physio-chemical changes in *Kobresia capillifolia* seedlings. *Plant Physiol Biochem* 194:15–28. <https://doi.org/10.1016/j.plaphy.2022.11.001>
- Tallesi M, Rijcken JF, Lammers T, Seevinck PR, Storm G, van Nostrum CF, Hennick WE (2009) Superparamagnetic iron oxide nanoparticles encapsulated in biodegradable thermoresponsive polymeric micelles: towards a targeted nanomedicine suitable for image-guided drug delivery. *Langmuir* 25(4):2060–2067. <https://doi.org/10.1021/la8036499>
- Tawfik MM, Mohamed MH, Sadak MS, Thaloath AT (2021) Iron oxide nanoparticles effect on growth, physiological traits and nutritional contents of *Moringa oleifera* grown in saline environment. *Bull Natl Res Cent* 45:177. <https://doi.org/10.1186/s42269-021-00624-9>
- Thanh DTM, Phuong NT, Hai DT, Giang HN, Thom NT, Nam PT, Dung NT, Giersig M, Osial M (2022) Influence of experimental conditions during synthesis on the physicochemical properties of the SPION/Hydroxyapatite nanocomposite for magnetic hyperthermia application. *Magnetochemistry* 8(90):1–17. <https://doi.org/10.3390/magnetochemistry8080090>
- Tymoszuk A, Miler N (2019) Silver and gold nanoparticles impact on *in vitro* adventitious organogenesis in chrysanthemum, gerbera and *Cape Primrose*. *Sci Hortic* 257:108766. <https://doi.org/10.1016/j.scienta.2019.108766>
- Wang XH, Li DP, Wang WJ, Feng QL, Ciu FZ, Xu YX, Song XH, van der Werf M (2003) Crosslinked collagen/chitosan matrix for artificial livers. *Biomaterials* 24:19, 3213–3220. [https://doi.org/10.1016/S0142-9612\(03\)00170-4](https://doi.org/10.1016/S0142-9612(03)00170-4)
- Wang X, Xie H, Wang P, Yin H (2023) Nanoparticles in plants: uptake, transport and physiological activity in leaf and root. *Materials* 16(8):3097. <https://doi.org/10.3390/ma16083097>
- Wierzbinski KR, Szymanski T, Rozwadowska N, Rybka JD, Zimna A, Zalewski T, Nowicka-Bauer K, Malcher A, Nowaczyk M, Krupinski M, Fiedorowicz M, Bogorodzki P, Grieb P, Giersig M, Kurpisz MK (2018) Potential use of superparamagnetic iron oxide nanoparticles for *in vitro* and *in vivo* bioimaging of human myoblasts. *Sci Rep* 8(1):3682. <https://doi.org/10.1038/s41598-018-22018-0>
- Zaid A, Ahmad B, Jaleel H, Wani SH, Hasanuzzaman M (2020) A critical review on iron toxicity and tolerance in plants: role of exogenous phytoprotectants. In: Aftab T, Hakeem KR (eds) *Plant micronutrients: deficiency and toxicity management*. Springer International Publishing, Cham, pp 83–99.
- Zhang X, Liu W, Lv Y, Tang J, Yang X, Bai J, Jin X, Zhou H (2022) Effects of drought stress during critical periods on the photosynthetic characteristics and production performance of Naked oat (*Avena nuda* L.). *Sci Rep* 12:11199. <https://doi.org/10.1038/s41598-022-15322-3>
- Zhao Y (2010) Auxin biosynthesis and its role in plant development. *Annu Rev Plant Biol* 61:49–64. <https://doi.org/10.1146/annurev-arplant-042809-112308>

Publisher's note Springer Nature remains neutral with regard to jurisdictional claims in published maps and institutional affiliations.

Springer Nature or its licensor (e.g. a society or other partner) holds exclusive rights to this article under a publishing agreement with the author(s) or other rightsholder(s); author self-archiving of the accepted manuscript version of this article is solely governed by the terms of such publishing agreement and applicable law.

Authors and Affiliations

Dariusz Kulus¹  · Alicja Tymoszuk¹ · Alicja Kulpińska¹ · Magdalena Osial²

✉ Dariusz Kulus
dariusz.kulus@pbs.edu.pl

Alicja Tymoszuk
alicja.tymoszuk@pbs.edu.pl

Alicja Kulpińska
mosial@ippt.pan.pl

¹ Laboratory of Horticulture, Department of Biotechnology, Faculty of Agriculture and Biotechnology, Bydgoszcz University of Science and Technology, Bernardyńska 6, 85-029 Bydgoszcz, Poland

² Institute of Fundamental Technological Research, Polish Academy of Sciences, Pawińskiego 5B, 02-106 Warsaw, Poland